Title	Nardilysin prevents amyloid plaque formation by enhancing α-secretase activity in an Alzheimer's disease mouse model.
Author(s)	Ohno, Mikiko; Hiraoka, Yoshinori; Lichtenthaler, Stefan F; Nishi, Kiyoto; Saijo, Sayaka; Matsuoka, Tatsuhiko; Tomimoto, Hidekazu; Araki, Wataru; Takahashi, Ryosuke; Kita, Toru; Kimura, Takeshi; Nishi, Eiichiro
Citation	Neurobiology of aging (2014), 35(1): 213-222
Issue Date	2014-01
URL	http://hdl.handle.net/2433/179454
Right	© 2014 Elsevier Inc.
Type	Journal Article
Textversion	author

Nardilysin prevents amyloid plaque formation by enhancing α-secretase activity in an Alzheimer's disease mouse model

Mikiko Ohno[1], Yoshinori Hiraoka[1], Stefan F. Lichtenthaler[2,3,4], Kiyoto Nishi[1], Sayaka Saijo[1], Tatsuhiko Matsuoka[1], Hidekazu Tomimoto[5], Wataru Araki[6], Ryosuke Takahashi[7], Toru Kita[8], Takeshi Kimura[1], and Eiichiro Nishi[1+]

[1]Department of Cardiovascular Medicine, Graduate School of Medicine, Kyoto University, Kyoto, Japan,

[2]German Center for Neurodegenerative Diseases (DZNE), site Munich, Germany

[3]Neuroproteomics, Klinikum rechts der Isar, Technische Universität München, 81675 Munich, Germany

[4]Munich Cluster for Systems Neurology (SyNergy), Munich, Germany

[5]Department of Neurology, Graduate School of Medicine, Mie University, Mie, Japan,

[6]National Institute of Neuroscience, NCNP, Tokyo, Japan

[7]Department of Neurology, Graduate School of Medicine, Kyoto University, Kyoto, Japan

[8]Kobe Medical Center General Hospital, Kobe, Japan

[+] Corresponding author. Tel.: +81 75 751 3187; Fax: +81 75 751 3203; E-mail: nishi@kuhp.kyoto-u.ac.jp

Amyloid-β (Aβ) peptide, the main component of senile plaques in patients with Alzheimer's disease (AD), is derived from proteolytic cleavage of amyloid precursor protein (APP) by β- and γ-secretases. Alpha-cleavage of APP by α-secretase has a potential to preclude the generation of Aβ because it occurs within the Aβ domain. We previously reported that a metalloendopeptidase, nardilysin (N-arginine dibasic convertase; NRDc) enhances α-cleavage of APP, which results in the decreased generation of Aβ *in vitro*. To clarify the *in vivo* role of NRDc in AD, we intercrossed transgenic mice expressing NRDc in the forebrain with AD model mice. Here we demonstrate that the neuron-specific overexpression of NRDc prevents Aβ deposition in the AD mouse model. The activity of α-secretase in the mouse brain was enhanced by the overexpression of NRDc, and was reduced by the deletion of NRDc. However, reactive gliosis adjacent to the Aβ plaques, one of the pathological features of AD, was not affected by the overexpression of NRDc. Taken together, our results indicate that NRDc controls Aβ formation through the regulation of α-secretase.

1. Introduction

Amyloid β peptide (Aβ) deposition in the extracellular region is one of the pathological hallmarks of Alzheimer's disease (AD). Aβ is derived from sequential cleavage of the amyloid precursor protein (APP), ectodomain shedding by β-secretase, and intramembrane cleavage by γ-secretase (Haass, 2004; Querfurth & LaFerla 2010; Selkoe & Schenk, 2003). As ectodomain shedding of APP by α-secretase occurs within the Aβ domain, it has the potential to preclude generation of the Aβ peptide. In addition, a secreted fragment of APP generated by α-cleavage (sAPP α) was shown to have neurotrophic and neuroprotective properties (Furukawa et al., 1996; Stein et al., 2004). An enhancement in α-secretase activity is considered to be a therapeutic approach for AD (Fahrenholz, 2007; Lichtenthaler, 2011). Several members of the ADAM (a disintegrin and metalloprotease) family, such as ADAM9, ADAM10, and ADAM17, have been reported to exhibit α-secretase activity (Kim et al., 2008). However, two recent studies, one using gene knockdown in primary neurons and the other using neurons derived from ADAM10 conditional knockout mice, demonstrated that the main α-secretase appears to be ADAM10 (Jorissen et al., 2010; Kuhn et al., 2010). Furthermore, ADAM10 overexpression in the AD mouse model reduced Aβ deposition, which indicated that activation of α-secretase is beneficial for the prevention of AD (Postina et al., 2004).

Nardilysin (EC 3.4.24.61, N-arginine dibasic convertase; NRDc) was initially identified as a metalloendopeptidase of the M16 family (Chesneau et al., 1994; Pierotti et al., 1994). We rediscovered NRDc as a specific binding partner of HB-EGF (Nishi et al., 2001), and demonstrated that NRDc enhances ectodomain shedding of HB-EGF through activation of ADAM17 (Nishi et al., 2006). Our subsequent studies showed that

ectodomain shedding of multiple membrane proteins such as TNF- α and APP is also enhanced by NRDc (Hiraoka et al., 2007; Hiraoka et al., 2008). Regarding APP, NRDc enhanced ADAM9-, ADAM10-, and ADAM17-induced α-cleavage, which resulted in the decreased generation of Aβ *in vitro* (Hiraoka et al., 2007).

We demonstrated using NRDc-deficient mice (*Nrd1$^{-/-}$*) that NRDc regulates myelination through the modulation of neuregulin1 (NRG1) shedding. Similar to APP, the membrane precursor of NRG1 is shown to be cleaved by ADAMs (α-secretase) and BACE1 (β-secretase) at two adjacent sites (Luo et al. 2011; Willem et al., 2006). We showed that ectodomain shedding of NRG1 is impaired in *Nrd1$^{-/-}$* fibroblasts and brains. Moreover, gain of function experiments in cells revealed that NRDc enhances ADAM17- and BACE1-mediated NRG1 shedding (Ohno et al., 2009). These findings suggested that NRDc is able to modulate both α- and β-secretase activity.

Here, to clarify the pathophysiological role of NRDc in AD, we evaluated the *in vivo* effect of NRDc overexpression or deletion on α- and β-secretase activity. We found that NRDc controls Aβ formation by mainly regulating α-secretase *in vivo*.

2. Methods

2.1. Animals

The background of mice used for all experiments was C57/BL6. Transgenic mice expressing mouse NRDc under the control of a forebrain neuron-specific CamkIIα promoter and NRDc-deficient mice (Acc.No. CDB0466K: http://www.cdb.riken.jp/arg/mutant%20mice%20list.html) were described previously (Ohno et al., 2009). APP transgenic mice (APP-Tg) overexpressing human APP695swe and the mutant presenillin1 (PS1-dE9) were obtained from Jackson Laboratories (B6C3-Tg (APPswe, PSEN1dE9) 85Dbo/Mmjax, stock number: 004462), and were intercrossed with NRDc-Tg to obtain double transgenic mice (APP/NRDc-Tg). Mice were housed in environmentally controlled rooms at the Institute of Laboratory Animals, Graduate School of Medicine, Kyoto University, under the Institute's guidelines for animal and recombinant DNA experiments. Three-month-old and one-year-old mice were deeply anesthetized with diethyl ether and euthanized. Mice were anesthetized and transcardially perfused with 4% paraformaldehyde in phosphate buffered saline for histological analysys, Mice were anesthetized and their brains were removed and immediately frozen in liquid nitrogen for biochemical analysis. Male mice were used for all experiments with the exception of Aβ42 ELISA, in which a similar number of male and female mice were analyzed.

2.2. Immunohistochemical staining, image capture and quantitative analysis

Immunohistochemical staining of mouse brain sections was performed as described previously (Ohno et al., 2009). Anti-GFAP (Z0334; DakoCytomation, Denmark), anti-F4/80 (BM8: BMA Biomedicals, Switzerland), anti-APP (A8717; Sigma, USA), anti-NRDc (#2371 raised in our laboratory) (Ohno et al., 2009), and anti-Aβ (6F/3D;

DakoCytomation, Denmark) antibodies were used. Pictures of immunostained sections were taken by a digital microscope (Keyence BZ9000). To analyze Aβ positive plaques, pictures of a whole brain section (three to four serial sections (7μm) at the same bregma level (Mouse Brain Atlas: bregma +1.3-1.8mm) per mouse) were obtained by combining 8-16 pictures at 40x magnitude using the image stitching function of BZ9000 (Supplementary Fig. 1A, and E). Plaque number, plaque surface area and whole brain surface area were measured by the dedicated software (Dynamic Cell Count System BZ-HIC) (Supplementary Fig. 1B-D, and F-H). The total surface area of the Aβ plaque was measured and expressed as a percentage of the total surface area of the whole brain (Plaque load). The number of F4/80- and GFAP-positive cells was also counted by the Dynamic Cell Count System. The value for F4/80-positive cells was expressed as a percentage of total DAPI-positive cells in the field.

2.3. Western blot analysis

The preparation of total cell extracts and Western blot analysis were performed as described previously (Nishi et al., 2006). Samples of conditioned media were prepared after concentration by Amicon Ultra Centrifugal Filter Units (Millipore). Samples of mouse brain extracts were prepared as described elsewhere (Kim et al., 2008). The anti-APP antibody (A8717; Sigma) was used to recognize the full-length and C83 fragment of APP. Anti-sAPPα and sAPPβ antibodies were described previously (Kuhn et al., 2010). The anti-APP C-terminal antibody 2C11 was also described previously (Kuhn et al., 2012). Anti-NRDc (mouse monoclonal #102 and rat monoclonal #1) antibodies were raised in our laboratory. The anti-β actin antibody (Santa Cruz) was used for the loading control.

2.4. RT-PCR

Total RNA extraction, cDNA synthesis, and quantitative real-time PCR were carried out as described previously (Ohno et al., 2009).

Mouse specific primers for RT-PCR are listed below. adam10: 5'- AGC ACC TTC AGG AAG CTC TGG, 3'-AAG TTT GTC CCC AGA TGT TG, adam17: 5'- CAC TTT GGT GCC TTT CGT CCT, 3'- CGT AGT CTG AGA GCA AAG AAT CAA CG, bace1: 5'- ACC ATC CTT CCT CAG CAA, 3'- GGG AAT GTT GTA GCC ACA, actb: 5'- CTG ACT GAC TAC CTC ATG AAG ATC CT,3'- CTT AAT GTC ACG CAC GAT TTC C, tnfa: 5'- AGC ACA GAA AGC ATG ATC CG, 3'- CCC GAA GTT CAG TAG ACA GAA CAG, gfap: 5'- TGT GGA GGG TCC TGT GTG TA, 3'- GTA GCC TGC TCC ACC TTC TG, f4/80: 5'- GCT GTG AGA TTG TGG AAG CA, 3'- CTG TAC CCA CAT GGC TGA TG, il6: 5'- CCA GTT GCC TTC TTG GGA CTG, 3'- CAG GTC TGT TGG GAG TGG TAT CC.

2.5. Measuring Aβ by sandwich ELISA

A frozen hemisphere was homogenized in four brain volumes of Tris-buffered saline (TBS) containing protease inhibitor cocktail (Complete Mini, Roche Diagnostic) and 2mM of 1,10-phenanthroline and was centrifuged at 100,000g for one hour at 4°C. The supernatant was saved as a TBS-soluble fraction. The pellet was resuspended in 6.25M guanidine HCL in 50mM Tris, pH8.0 and nutated for two hours at RT, followed by a second centrifugation at 20,800g for 20 min at 4°C. The supernatant was saved as a guanidine-extracted fraction (GuHCL-soluble). The concentration of Aβ42 in the TBS- or GuHCL-soluble fraction of brain extracts was measured by sandwich ELISA as described previously (Hiraoka et al., 2007).

2.6. Measuring IL-6 by sandwich ELISA

Protein expression levels of mouse IL-6 in brain extracts were measured using the

DuoSet ELISA Development kit (R&D Systems, Inc.) according to the manufacturer's protocol.

2.7. β-Secretase activity assay

β-Secretase activity in brain extracts was measured using the β-Secretase activity kit (R&D systems) according to the manufacturer's protocol.

2.8. Cell culture and transfections

HEK293 cells expressing APP (HEK293-APP) were cultured in Dulbecco's modified Eagle's medium supplemented with 10% fetal bovine serum and 200 μg/ml G418 in a humidified atmosphere of 95% air, 5% CO_2 at 37 °C (Murayama et al., 2006). Transfections of plasmid DNA and siRNA were carried out using X-treme GENE (Roche Diagnostics) according to the manufacturer's protocol. The sequences for siRNA duplexes against mouse NRDc and human ADAM10 were described previously (Hiraoka et al., 2007).

2.9. Statistical analysis

Data are represented as the mean +/- s.e.m. Statistical analysis (unpaired Student's two-tailed *t* test) was performed using the Statview software package (SAS institute).

3. Results

3.1. *Enhanced NRDc expression reduces Aβ deposition in the forebrain of the AD mouse model*

We generated transgenic mice expressing mouse NRDc under the control of a forebrain neuron-specific CamkIIα promoter (NRDc-Tg) (Ohno et al., 2009). Although NRDc-Tg mice show hypermyelination especially in the corpus callosum, they exhibited no behavioral abnormalities throughout their life span. To examine the pathophysiological effects of NRDc overexpression on AD progression, we intercrossed NRDc-Tg with AD model mice (APP-Tg: transgenic mice expressing APP695swe and a mutant presenillin1 (PS1-dE9)) and analyzed their brains at one year of age. As shown in Figure 1A, NRDc expression was obviously higher in neurons of the cortex and hippocampus in APP/NRDc-Tg mice than in APP-Tg mice. Immunoblot analysis revealed that NRDc protein expression in the forebrain of APP/NRDc-Tg mice was two- to three-fold higher than that in APP-Tg mice (Fig. 1B). Consistent with these results, mRNA expression levels of NRDc in APP/NRDc-Tg mice were three times higher than those in APP-Tg mice (Fig. 1C). On the other hand, protein expression levels of the full length of APP (APP-FL) and its mRNA levels were not affected by the overexpression of NRDc (Fig. 1B and data not shown). We also examined the mRNA levels of major candidates of α- and β-secretase in the forebrain. No significant differences were observed in *adam10, adam17,* or *bace1* mRNA levels between APP-Tg and APP/NRDc-Tg mice (data not shown).

Amyloid plaques were detected by immunohistochemistry using an antibody for Aβ (Fig. 2A and B), and the number and surface area of Aβ positive plaques were quantitated in a whole brain section (Supplementary Fig. 1). The average number of Aβ

plaques was significantly lower in APP/NRDc-Tg mice than that in APP-Tg mice (APP-Tg; 822.1+/-101.5, APP/NRDc-Tg; 322.4+/-69.2, average plaque number +/- SE per section, p<0.01, APP-Tg; 727.8, APP/NRDc-Tg; 290.7, median value, n=7: APP-Tg, n=6: APP/NRDc-Tg) (Fig. 2C). While the average surface area of each plaque was not significantly different between APP-Tg and APP/NRDc-Tg mice (data not shown), the plaque load (total plaque surface area/total brain surface area) was significantly lower in APP/NRDc-Tg mice (APP-Tg; 0.34+/-0.058, APP/NRDc-Tg; 0.12+/-0.033, average plaque load +/- SE, p<0.05, APP-Tg; 0.24, APP/NRDc-Tg; 0.10, median value, n=7: APP-Tg, n=6: APP/NRDc-Tg) (Fig. 2D). We also quantitatively analyzed the amount of Aβ using an ELISA, specific for Aβ42. The concentration of Aβ42 in both soluble (TBS-soluble) and insoluble (GuHCL-soluble) fractions of forebrain extracts was significantly lower in APP/NRDc-Tg mice than that in APP/Tg mice (Fig. 2E, and F). These results clearly demonstrated that the enhanced expression of NRDc reduces Aβ deposition *in vivo*.

3.2. *NRDc regulates α-secretase activity in vitro and in vivo*

To assess the activity of α-secretase, we used an antibody (4B4) that specifically recognizes the α-cleavage site of APP (Fig. 3A). This antibody detects the C-terminal ending of sAPPα, and thus detects neither the full-length of APP nor shorter forms of sAPP, such as sAPPβ (Kuhn et al., 2010). We first performed gene knockdown of ADAM10 in HEK293 cells stably overexpressing APP (HEK293-APP) (Murayama et al., 2006) to assess the role of ADAM10 as α-secretase in these cells. As expected, secreted sAPPα in the conditioned medium and the C-terminal remnant of APP (C83) were markedly reduced in ADAM10-knocked down cells (Fig. 3B), which indicated

that ADAM10 is the main α-secretase in HEK293-APP cells. Gene knockdown of NRDc in HEK293-APP cells also showed a clear reduction in secreted sAPPα in the conditioned medium and C-terminal remnant of APP (C83) (Fig.3C). Competition between α- and β-secretase was not observed in both cases because sAPPβ levels were not increased either by NRDc knockdown or ADAM10 knock-down (Fig. 3B, and C), in agreement with a previous report (Colombo et al., 2012). Furthermore, co-precipitation of NRDc and ADAM10 was detected in HEK293-APP cells (Fig. 3D), which suggested that NRDc physically and functionally interacts with ADAM10 and regulates its α-secretase activity.

To examine the *in vivo* effect of NRDc on α-cleavage, forebrain extracts were analyzed by immunoblotting with the anti-sAPPα antibody. As shown in Figures 4A and B, the amount of sAPPα was clearly higher in APP/NRDc-Tg mice than that in APP-Tg mice, indicating that the overexpression of NRDc enhances α-secretase activity *in vivo*. To examine the competitive effect of enhanced α-secretase activity on β-secretase in APP/NRDc-Tg mice, sAPPβ and β-secretase activity levels were evaluated in brain extracts by immunoblotting and a peptide cleavage assay, respectively. While there were no statistically significant differences between APP-Tg and APP/NRDc-Tg mice, both sAPPβ and β-secretase activity levels showed clear tendencies to be lower in APP/NRDc-Tg mice compared with APP-Tg mice (Fig. 4B and C).

To further define the *in vivo* role of NRDc in the regulation of α-and β-secretase activity, we examined endogenous sAPPα and sAPPβ protein levels in $Nrd1^{-/-}$ forebrains. sAPPα protein levels were markedly lower in $Nrd1^{-/-}$ brains than in $Nrd1^{+/+}$ brains, whereas sAPPβ was not clearly altered in $Nrd1^{-/-}$ brains (Fig. 4D, and E). Similar to the *in vitro* results of NRDc knockdown experiments (Fig. 3C),

competition between α- and β-secretase did not occur in $Nrd1^{-/-}$ brains. Taken together, our gain of function and loss of function approaches *in vivo* indicated that the expression level of NRDc strongly correlated with α-secretase activity. Our results also suggested that NRDc overexpression reduces Aβ deposition via the enhancement of α-secretase activity and a possible competitive inhibition of β-secretase *in vivo*.

To assess whether NRDc altered the Aβ production prior to plaque formation, we measured Aβ using ELISA in 3-month-old mice. At this early phase, no significant differences were observed in either soluble or insoluble Aβ between APP-Tg and APP/NRDc-Tg mice (Supplementary Fig. 2A). The amount of Aβ in 3-month-old APP-Tg mice was approximately 1/10 and 1/1000 that of 1-year-old mice in the soluble and insoluble fractions, respectively. Consistent with these results, no significant alterations were detected in the amount of sAPPα and sAPPβ between the two genotypes; however sAPPα tended to be higher and sAPPβ tended to be lower in APP/NRDc-Tg mice (Supplementary Fig. 2B, and C).

3.3. NRDc overexpression does not affect reactive gliosis in the AD mouse model

Although reactive gliosis adjacent to plaques is one of the pathological features of AD, the role of an inflammatory response in AD still remains controversial (Morgan et al., 2005; Wyss-Coray, 2006). As the pro-inflammatory role of NRDc has been suggested (Hiraoka et al., 2008; Kanda et al., 2012), we examined the effect of NRDc on inflammatory responses that occurred in the AD mouse model. First, we examined the mRNA expression levels of TNF-α and IL-6, inflammatory cytokines, and those of GFAP and F4/80, markers of responsive astrocytes and microglia, at 3 months and 1 year of age **(**Fig. 5A and B**)**. No significant difference was observed in these mRNA

levels at one year of age (TNF-α mRNA expression was not detectable), whereas IL-6 mRNA levels only were significantly higher in APP/NRDc-Tg mice than in APP-Tg mice at 3 months of age (Fig. 5A, and B). To confirm an increase in protein levels, we measured IL-6 levels in total brain extracts using ELISA. However, no significant differences were observed in IL-6 protein levels between APP-Tg and APP/NRDc-Tg mice both at 3 months and 1 year of age (Fig. 5C). We then evaluated the extent of microgliosis and astrogliosis by immunohistochemistry using the anti F4/80 antibody and anti-glial fibrillary acidic protein (GFAP) antibody, respectively (Fig. 5D, and F). No alteration was observed in the number of either F4/80-positive or GFAP-positive cells between APP-Tg and APP/NRDc-Tg mice at both 3 months and 1 year old of age (Fig. 5E, and G), indicating that NRDc overexpression does not affect reactive gliosis in the AD mouse model.

Discussion

Our findings provide the first *in vivo* evidence that a metalloendopeptidase NRDc prevents amyloid plaque formation in the AD mouse model. Forebrain neuron-specific NRDc overexpression increased the level of sAPPα and reduced Aβ deposition, indicating that NRDc precludes Aβ deposition through the activation of α-secretases. NRDc overexpression in NRDc-Tg mice was only modest (2- to 3-fold higher than that in wild-type mice), suggesting the physiological role of NRDc in the regulation of α-secretase. In contrast, the level of sAPPα was clearly lower in $Nrd1^{-/-}$ brains than in $Nrd1^{+/+}$ brains. These results suggest that α-secretase activity is critically regulated by the expression level of NRDc *in vivo*.

We identified NRDc as a cell surface binding partner of HB-EGF (Nishi et al., 2001). We subsequently demonstrated that NRDc enhanced ectodomain shedding of not only HB-EGF, but also of APP, TNF-α, and neuregulin-1 (NRG1) (Hiraoka et al., 2007; Hiraoka et al., 2008; Nishi et al., 2006; Ohno et al., 2009). In cell culture experiments, NRDc enhanced ADAM9-, ADAM10-, and ADAM17-induced α-cleavage, which resulted in the decreased generation of Aβ. We previously demonstrated the binding of ADAM17 and NRDc (Nishi et al., 2006). Furthermore, the recombinant protein of NRDc enhances ADAM17-mediated α-cleavage in a peptide cleavage assay (Hiraoka et al., 2007), while NRDc itself, which has endopeptidase activity, does not cleave Aβ at the α-cleavage site (Hiraoka et al., 2007). NRDc may activate ADAM10 in a similar manner because we demonstrate here the complex formation of NRDc and ADAM10. The activation of α-secretase is considered to be a therapeutic approach for AD (Fahrenholz, 2007; Lichtenthaler, 2011). This hypothesis was supported by the finding that ADAM10 overexpression reduced Aβ deposition in the AD mouse model (Postina

14

et al., 2004). We show here that NRDc, an activator of ADAMs, diminished amyloid plaque load *in vivo*, which further supports this hypothesis.

We recently reported that NRDc regulates myelination in the central and peripheral nervous system by regulating NRG1 shedding. NRG1 shares a unique characteristic with APP in which both are cleaved by ADAMs and BACE1 at two different sites in the juxtamembrane region (Luo et al.; Willem et al., 2006). We demonstrated that the overexpression of NRDc enhances ADAM17- and BACE1-mediated NRG1 shedding in a cell-based assay. Interestingly, NRDc has been shown to potentiate ADAM17-mediated NRG1 cleavage at the cell surface, whereas NRDc enhanced BACE1 cleavage of NRG1 in intracellular compartments (Ohno et al., 2009). These findings are in line with a previous study, which showed that α-secretase cleavage mainly occurs at the plasma membrane while β-secretase cleavage mainly occurs in the endosome (Thinakaran & Koo, 2008). In the present study, we examined the *in vivo* effect of NRDc on β-secretase activity in the AD mouse model. Importantly, β-secretase activity in the brain tended to be reduced rather than enhanced by the overexpression of NRDc, which is most probably due to the competitive effect of enhanced α-secretase activity. β-secretase activity was not affected by the deletion of NRDc *in vivo*, although the activity of α-secretase was clearly decreased in *Nrd1*^{−/−} brains. β-secretase activity was also not altered by gene knockdown of NRDc in the cell-based assay. These findings indicate that NRDc is not critically involved in the regulation of β-secretase. We previously demonstrated that NRDc appears to be involved in the protein maturation of BACE1 (Ohno et al., 2009). One possible explanation for the discrepancy between NRG1 and APP could be that NRG1 shedding, but not APP shedding is enhanced by NRDc-mediated modulation of BACE1.

The roles of NRDc in inflammation have been suggested previously. For example, NRDc has been shown to enhance ectodomain shedding of TNF-α (Hiraoka et al., 2008), and stimulates the expression of IL-6 in gastric cancer cells, resulting in the promotion of cancer growth (Kanda et al., 2012). IL-6 and other inflammatory cytokines such as IL-1 and TNF-α were shown to be elevated in the brains of AD patients, suggesting the detrimental effect of these cytokines on the disease (Wyss-Coray, 2006). However, a recent report demonstrated that IL-6 overexpression attenuates Aβ deposition probably through enhanced microglia-mediated phagocytosis (Chakrabarty et al., 2009). The enhanced expression of NRDc in the forebrain increased IL-6 mRNA levels, but not those of TNF-α, at an early stage of AD (three months), which was not accompanied with an increase in the IL-6 protein. Since we have shown that NRDc knockdown in several cancer cell lines decreases IL-6 mRNA and protein levels (Kanda et al., 2012), the dissociation of mRNA and protein levels in brains could be a tissue-specific matter. Consistent with the unchanged protein expression level of IL-6, no alteration in responsive gliosis was observed between the two genotypes at the early or late stage of the disease (one year). These results indicate that inflammation-mediated Aβ clearance may not be involved in the reduction of Aβ plaques in APP/NRDc-Tg mice.

Maes et al. analyzed gene expressions of blood mononuclear cells derived from AD patients and found that NRDc is upregulated in AD patients compared to age-matched normal controls (Maes et al., 2007). Our preliminary findings using autopsy samples also showed that NRDc expression in the cortical neurons of AD patients tends to be higher than that in control patients (data not shown). Given these results on human, we have to carefully interpret our findings in AD model mice. The

increase of NRDc in AD patients could be a rescue response of the brain to the damage by Aβ, which might not be sufficient to prevent the disease progression. On the other hand, we previously showed that NRDc is highly expressed in mouse brains at the early postnatal stage, but is expressed at a very low level in adult mice (Hiraoka et al., 2007; Ohno et al., 2009). NRDc expression in the human brain may also be dynamically regulated in physiological and pathological processes. However, NRDc is highly expressed in the transgenic mouse model APP/NRDc-Tg throughout the life period from around postnatal day 5. The constantly high expression of NRDc may affect Aβ pathology differently than it does in human AD. Future studies using a more sophisticated mouse model, such as an inducible tissue-specific knockout or overexpression of NRDc, will improve our understanding on the role of NRDc in AD.

We established a highly sensitive ELISA for NRDc (Kanda et al., 2012), which enables us to measure NRDc in the serum or cerebrospinal fluid of AD patients. It is also important to further examine the expression levels of neuronal NRDc in AD autopsy samples. These data on human AD, together with mouse data, will clarify the pathophysiological roles of NRDc in AD. While a role of NRDc in human AD has not been sufficiently clarified, our finding that NRDc is a crucial *in vivo* regulator for α-secretase activity may improve our understanding on the pathogenesis of AD.

Disclosure statement

There are no actual or potential conflicts of interest.

All experiments with mice followed the Institute's guidelines for animals and were approved by the Institute of Laboratory Animals, Graduate School of Medicine, Kyoto University.

References

Chakrabarty P, Jansen-West K, Beccard A, Ceballos-Diaz C, Levites Y, Verbeeck C, Zubair AC, Dickson D, Golde TE, Das P (2009) Massive gliosis induced by interleukin-6 suppresses Abeta deposition in vivo: evidence against inflammation as a driving force for amyloid deposition. *FASEB J* **24:** 548-559

Chesneau V, Pierotti AR, Prat A, Gaudoux F, Foulon T, Cohen P (1994) N-arginine dibasic convertase (NRD convertase): a newcomer to the family of processing endopeptidases. An overview. *Biochimie* **76:** 234-240

Colombo A, Wang H, Kuhn PH, Page R, Kremmer E, Dempsey PJ, Crawford HC, Lichtenthaler SF (2012) Constitutive alpha- and beta-secretase cleavages of the amyloid precursor protein are partially coupled in neurons, but not in frequently used cell lines. *Neurobiology of disease* **49C:** 137-147

Fahrenholz F (2007) Alpha-secretase as a therapeutic target. *Curr Alzheimer Res* **4:** 412-417

Furukawa K, Sopher BL, Rydel RE, Begley JG, Pham DG, Martin GM, Fox M, Mattson MP (1996) Increased activity-regulating and neuroprotective efficacy of alpha-secretase-derived secreted amyloid precursor protein conferred by a C-terminal heparin-binding domain. *J Neurochem* **67:** 1882-1896

Haass C (2004) Take five--BACE and the gamma-secretase quartet conduct Alzheimer's amyloid beta-peptide generation. *EMBO J* **23:** 483-488

Hiraoka Y, Ohno M, Yoshida K, Okawa K, Tomimoto H, Kita T, Nishi E (2007) Enhancement of alpha-secretase cleavage of amyloid precursor protein by a metalloendopeptidase nardilysin. *J Neurochem* **102:** 1595-1605

Hiraoka Y, Yoshida K, Ohno M, Matsuoka T, Kita T, Nishi E (2008) Ectodomain shedding of TNF-alpha is enhanced by nardilysin via activation of ADAM proteases. *Biochem Biophys Res Commun* **370:** 154-158

Jorissen E, Prox J, Bernreuther C, Weber S, Schwanbeck R, Serneels L, Snellinx A, Craessaerts K, Thathiah A, Tesseur I, Bartsch U, Weskamp G, Blobel CP, Glatzel M, De Strooper B, Saftig P (2010) The disintegrin/metalloproteinase ADAM10 is essential for the

establishment of the brain cortex. *J Neurosci* **30:** 4833-4844

Kanda K, Komekado H, Sawabu T, Ishizu S, Nakanishi Y, Nakatsuji M, Akitake-Kawano R, Ohno M, Hiraoka Y, Kawada M, Kawada K, Sakai Y, Matsumoto K, Kunichika M, Kimura T, Seno H, Nishi E, Chiba T (2012) Nardilysin and ADAM proteases promote gastric cancer cell growth by activating intrinsic cytokine signalling via enhanced ectodomain shedding of TNF-alpha. *EMBO Mol Med* **4:** 396-411

Kim ML, Zhang B, Mills IP, Milla ME, Brunden KR, Lee VM (2008) Effects of TNFalpha-converting enzyme inhibition on amyloid beta production and APP processing in vitro and in vivo. *J Neurosci* **28:** 12052-12061

Kuhn PH, Koroniak K, Hogl S, Colombo A, Zeitschel U, Willem M, Volbracht C, Schepers U, Imhof A, Hoffmeister A, Haass C, Rossner S, Brase S, Lichtenthaler SF (2012) Secretome protein enrichment identifies physiological BACE1 protease substrates in neurons. *EMBO J* **31:** 3157-3168

Kuhn PH, Wang H, Dislich B, Colombo A, Zeitschel U, Ellwart JW, Kremmer E, Rossner S, Lichtenthaler SF (2010) ADAM10 is the physiologically relevant, constitutive alpha-secretase of the amyloid precursor protein in primary neurons. *EMBO J* **29:** 3020-3032

Lichtenthaler SF (2011) Alpha-secretase in Alzheimer's disease: molecular identity, regulation and therapeutic potential. *J Neurochem* **116:** 10-21

Luo X, Prior M, He W, Hu X, Tang X, Shen W, Yadav S, Kiryu-Seo S, Miller R, Trapp BD, Yan R (2011) Cleavage of neuregulin-1 by BACE1 or ADAM10 protein produces differential effects on myelination. *J Biol Chem* **286:** 23967-23974

Maes OC, Xu S, Yu B, Chertkow HM, Wang E, Schipper HM (2007) Transcriptional profiling of Alzheimer blood mononuclear cells by microarray. *Neurobiology of aging* **28:** 1795-1809

Morgan D, Gordon MN, Tan J, Wilcock D, Rojiani AM (2005) Dynamic complexity of the microglial activation response in transgenic models of amyloid deposition: implications for Alzheimer therapeutics. *J Neuropathol Exp Neurol* **64:** 743-753

Murayama KS, Kametani F, Saito S, Kume H, Akiyama H, Araki W (2006) Reticulons RTN3 and RTN4-B/C interact with BACE1 and inhibit its ability to produce amyloid beta-protein. *Eur J Neurosci* **24**: 1237-1244

Nishi E, Hiraoka Y, Yoshida K, Okawa K, Kita T (2006) Nardilysin enhances ectodomain shedding of heparin-binding epidermal growth factor-like growth factor through activation of tumor necrosis factor-alpha-converting enzyme. *J Biol Chem* **281**: 31164-31172

Nishi E, Prat A, Hospital V, Elenius K, Klagsbrun M (2001) N-arginine dibasic convertase is a specific receptor for heparin-binding EGF-like growth factor that mediates cell migration. *EMBO J* **20**: 3342-3350

Ohno M, Hiraoka Y, Matsuoka T, Tomimoto H, Takao K, Miyakawa T, Oshima N, Kiyonari H, Kimura T, Kita T, Nishi E (2009) Nardilysin regulates axonal maturation and myelination in the central and peripheral nervous system. *Nat Neurosci* **12**: 1506-1513

Pierotti AR, Prat A, Chesneau V, Gaudoux F, Leseney AM, Foulon T, Cohen P (1994) N-arginine dibasic convertase, a metalloendopeptidase as a prototype of a class of processing enzymes. *Proc Natl Acad Sci U S A* **91**: 6078-6082

Postina R, Schroeder A, Dewachter I, Bohl J, Schmitt U, Kojro E, Prinzen C, Endres K, Hiemke C, Blessing M, Flamez P, Dequenne A, Godaux E, van Leuven F, Fahrenholz F (2004) A disintegrin-metalloproteinase prevents amyloid plaque formation and hippocampal defects in an Alzheimer disease mouse model. *J Clin Invest* **113**: 1456-1464

Querfurth HW, LaFerla FM (2010) Alzheimer's disease. *N Engl J Med* **362**: 329-344

Selkoe DJ, Schenk D (2003) Alzheimer's disease: molecular understanding predicts amyloid-based therapeutics. *Annu Rev Pharmacol Toxicol* **43**: 545-584

Stein TD, Anders NJ, DeCarli C, Chan SL, Mattson MP, Johnson JA (2004) Neutralization of transthyretin reverses the neuroprotective effects of secreted amyloid precursor protein (APP) in APPSW mice resulting in tau phosphorylation and loss of hippocampal neurons: support for the amyloid hypothesis. *J Neurosci* **24**: 7707-7717

Thinakaran G, Koo EH (2008) Amyloid precursor protein trafficking, processing, and

function. *J Biol Chem* **283:** 29615-29619

Willem M, Garratt AN, Novak B, Citron M, Kaufmann S, Rittger A, DeStrooper B, Saftig P, Birchmeier C, Haass C (2006) Control of peripheral nerve myelination by the beta-secretase BACE1. *Science* **314:** 664-666

Wyss-Coray T (2006) Inflammation in Alzheimer disease: driving force, bystander or beneficial response? *Nat Med* **12:** 1005-1015

Figure legends

Figure 1) Increased NRDc protein and mRNA levels in the forebrain of APP/NRDc-Tg mice

(A) Immunostaining of NRDc in the cortex (upper panel) and hippocampus (lower panel) of APP-Tg (left panel) and APP/NRDc-Tg mice (right panel). NRDc is up-regulated in the neurons of APP/NRDc-Tg brain sections. Scale bar: 100μm

(B) Immunoblot analysis of total brain extracts from non-transgenic (Non-Tg), NRDc-Tg, APP-Tg, and APP/NRDc-Tg mice.

(C) *Nrd1* mRNA expression levels in the whole brains of APP-Tg and APP/NRDc-Tg mice. n=3 / genotype. The expression levels of each mRNA were standardized by that of β-actin. Data represents the mean +/- s.e.m; * indicates P<0.05

Figure 2) Enhanced NRDc expression reduces Aβ deposition in the forebrain of the AD mouse model

(A,B) Immunostaining of Aβ in the brain sections of APP-Tg and APP/NRDc-Tg mice. Whole brain sections (A) and a higher magnification view of the hippocampus at the same bregma level (B) are shown. Scale bar: 2mm (A), 250μm (B)

(C) Quantitation of Aβ positive plaque numbers in forebrain sections. At least four sections of a whole brain at the same bregma level were analyzed. Plaque number per a section was averaged by mouse and the average value of each mouse was used for statistical analysis. n=7: APP-Tg, n=6: APP/NRDc-Tg. Data represents the mean +/- s.e.m; **p<0.01.

 (D) Quantitation of Aβ plaque load (total plaque surface area / whole brain surface area) in forebrain sections, which was analyzed in a similar manner to plaque number

(C). n=7: APP-Tg, n=6: APP/NRDc-Tg. Data represents the mean +/- s.e.m; *p<0.05.

(E, F) Measurement of the Aβ42 peptide in the soluble and insoluble fractions of whole brain extracts by ELISA. (n=11 (male; 6, female; 5) for APP-Tg,　n=12 (male; 6, female; 6) for APP/NRDc-Tg. Data represents the mean +/- s.e.m; *p<0.01.

Figure 3) NRDc regulates α-secretase activity *in vitro*

(A) Schematic diagram of APP-FL, sAPPα, sAPPβ, C83, and C99. The black box denotes Aβ. APP-FL: full length of APP, sAPPα, sAPPβ: α or β-secretase-cleaved APP ectodomain.

(B, C) Immunoblot analysis of the cell extracts and conditioned medium (CM) of HEK 293 cells stably expressing APP in which ADAM10 (B) or NRDc (C) was knocked down, respectively. (D) Immunoprecipitation of co-transfected cell lysates with an antibody to HA revealed a complex of NRDc (V5) and ADAM10 (HA).

Regarding pictures of gels, comparable data were obtained in at least 3 independent experiments, and a representative gel is shown.

Figure 4) NRDc regulates α-secretase activity *in vivo*

(A, B) Representative immunoblot analysis of brain extracts from APP-Tg (left panel) and APP/NRDc-Tg mice (right panel) (n=3/genotype). The quantification of signals by densitometry is shown in (B). The intensity of bands relative to that of β-actin was arbitrarily set at one in APP-Tg mice. n=5/genotype, *P<0.01

(C) β-secretase activity in brain extracts analyzed by the peptide cleavage assay. n=11 for APP-Tg, n=12 for APP/NRDc-Tg. Data represents the mean +/- s.e.m; p=0.16.

(D, E) Representative immunoblot analysis of brain extracts from wild-type ($Nrd1^{+/+}$: left panel) and $Nrd1^{-/-}$ mice (right panel) (one-year-old, n=3/genotype). The quantification of signals by densitometry is shown in (E). The intensity of bands relative to that of β-actin was arbitrarily set at one in $Nrd1^{+/+}$. n=5/genotype, *P<0.01

Figure 5) NRDc overexpression does not affect reactive gliosis in the AD mouse model

(A, B) Analysis of the mRNA expression of inflammatory cytokines and markers of reactive gliosis at 3 months (A) and 1 year of age (B). n=3 / genotype. Expression levels of each mRNA were standardized to that of β-actin. Data represents the mean +/- s.e.m; * indicates P<0.05.

(C) Analysis of the IL-6 protein in forebrain lysates by ELISA. 3-month-old: n=8/genotype, p=0.46, 1 year old: n=4/genotype, p=0.64. Data represents the mean +/-s.e.m.

(D) Immunohistochemical detection of F4/80 in the cortex of APP-Tg and APP/NRDc-Tg mice at one year of age. Scale bar: 50μm.

(E) Quantitation of F4/80-positive cells. Percentage of F4/80-positive cells per DAPI positive cells was analyzed for 15-20 fields in 3 serial sections per mouse. n=3/genotype, Data represents the mean +/- s.e.m.; P=0.86 for 3-month-old, P=0.24 for 1-year-old mice.

(F) Immunohistochemical detection of GFAP (green) and Aβ (red) in the cortex. Scale bar: 50μm

(G) Quantitation of GFAP-positive cells.   GFAP-positive cell numbers in the cortex and hippocampus were analyzed in 6 sections at the same bregma level. n=3/genotype. Data
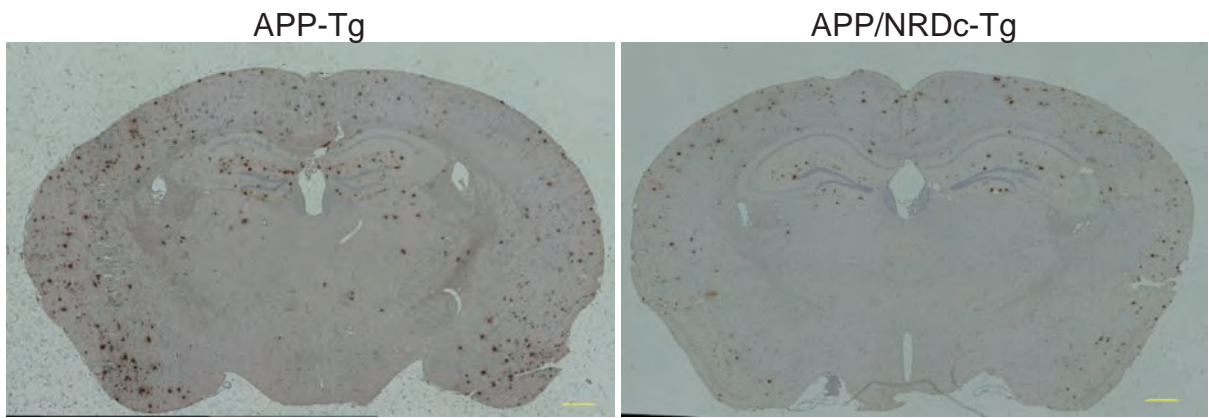
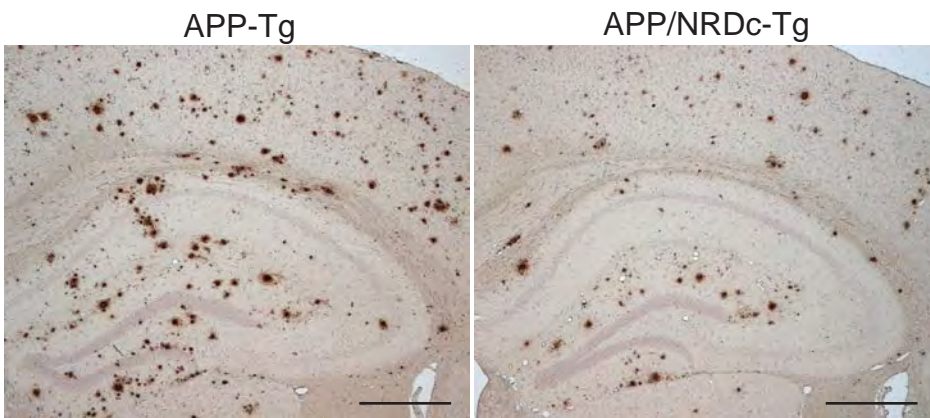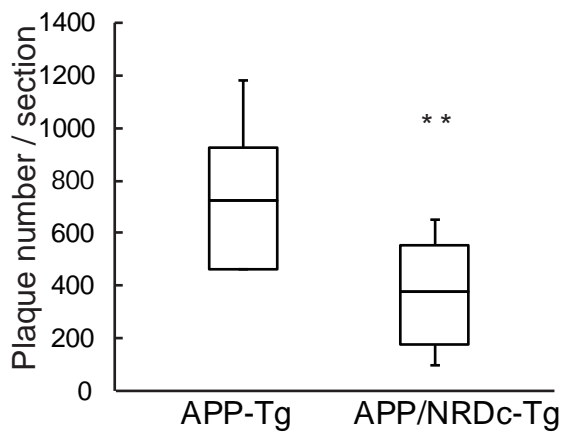represents the mean +/- s.e.m; P=0.94.

<Figure1> Ohno M. et al.

A

APP-Tg APP/NRDc-Tg

Cortex

Hippocampus

B

Non-Tg NRDc-Tg APP-Tg APP/NRDc-Tg

NRDc

APP

β-actin

C

NRDc

Relative mRNA expression

3.5
3
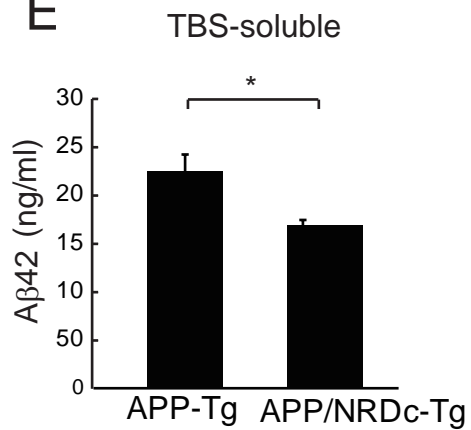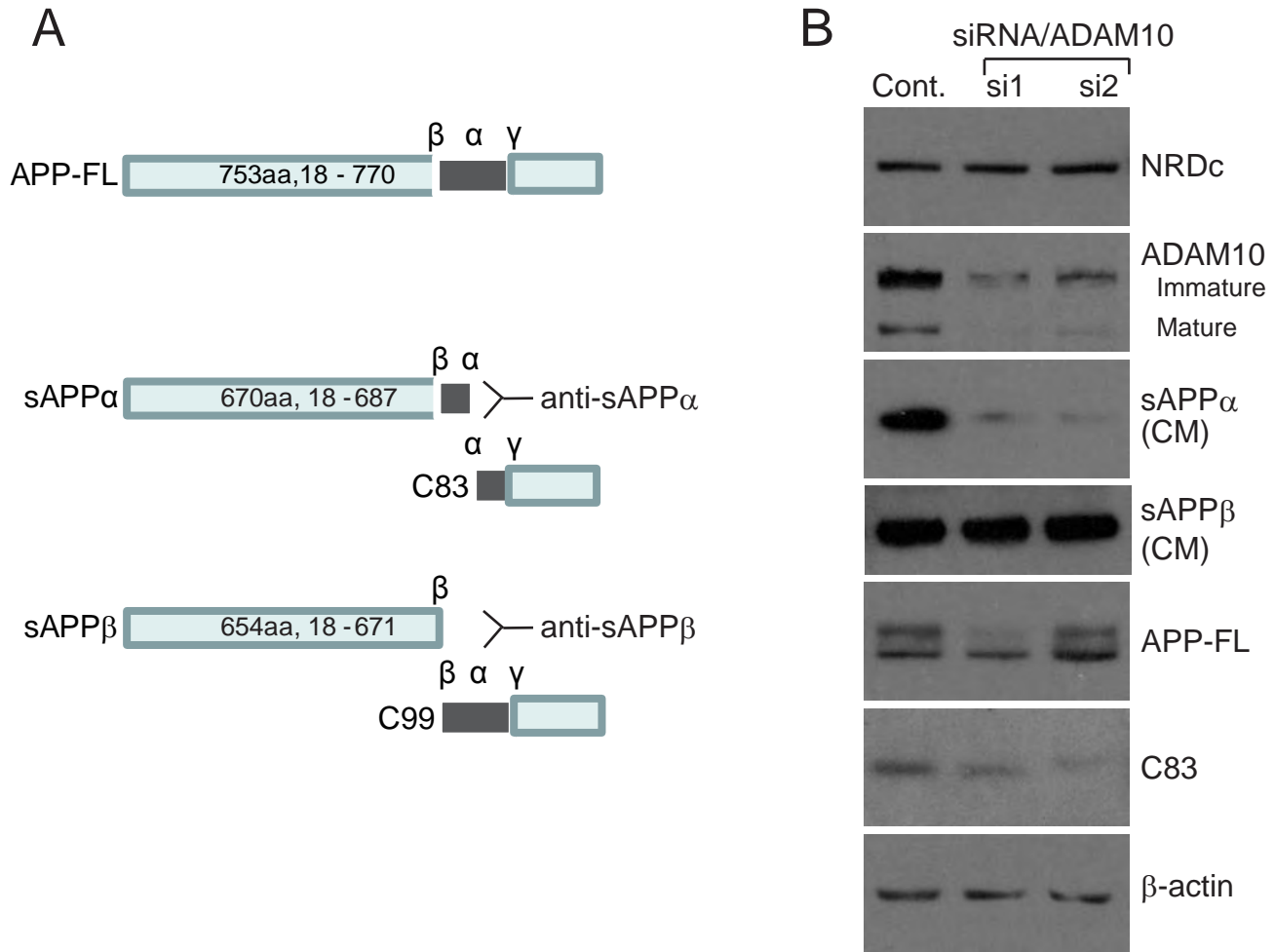2.5
2
1.5
1
0.5
0

*

APP-Tg   APP/NRDc-Tg

<Figure2> Ohno M. et al.

<Figure3> Ohno M. et al.

A

APP-FL — 753aa,18 - 770 | β α γ

sAPPα — 670aa, 18 -687 | β α — anti-sAPPα

C83 — α γ

sAPPβ — 654aa, 18 - 671 | β — anti-sAPPβ

C99 — β α γ

B

siRNA/ADAM10

Cont. si1 si2

NRDc

ADAM10
Immature
Mature

sAPPα (CM)

sAPPβ (CM)

APP-FL

C83

β-actin

C

siRNA/NRDc

Cont. si1 si2

NRDc

sAPPα (CM)

sAPPβ (CM)

APP-FL

C83

β-actin

D

NRDc (V5) − + − +   IB
ADAM10 (HA) − − + +

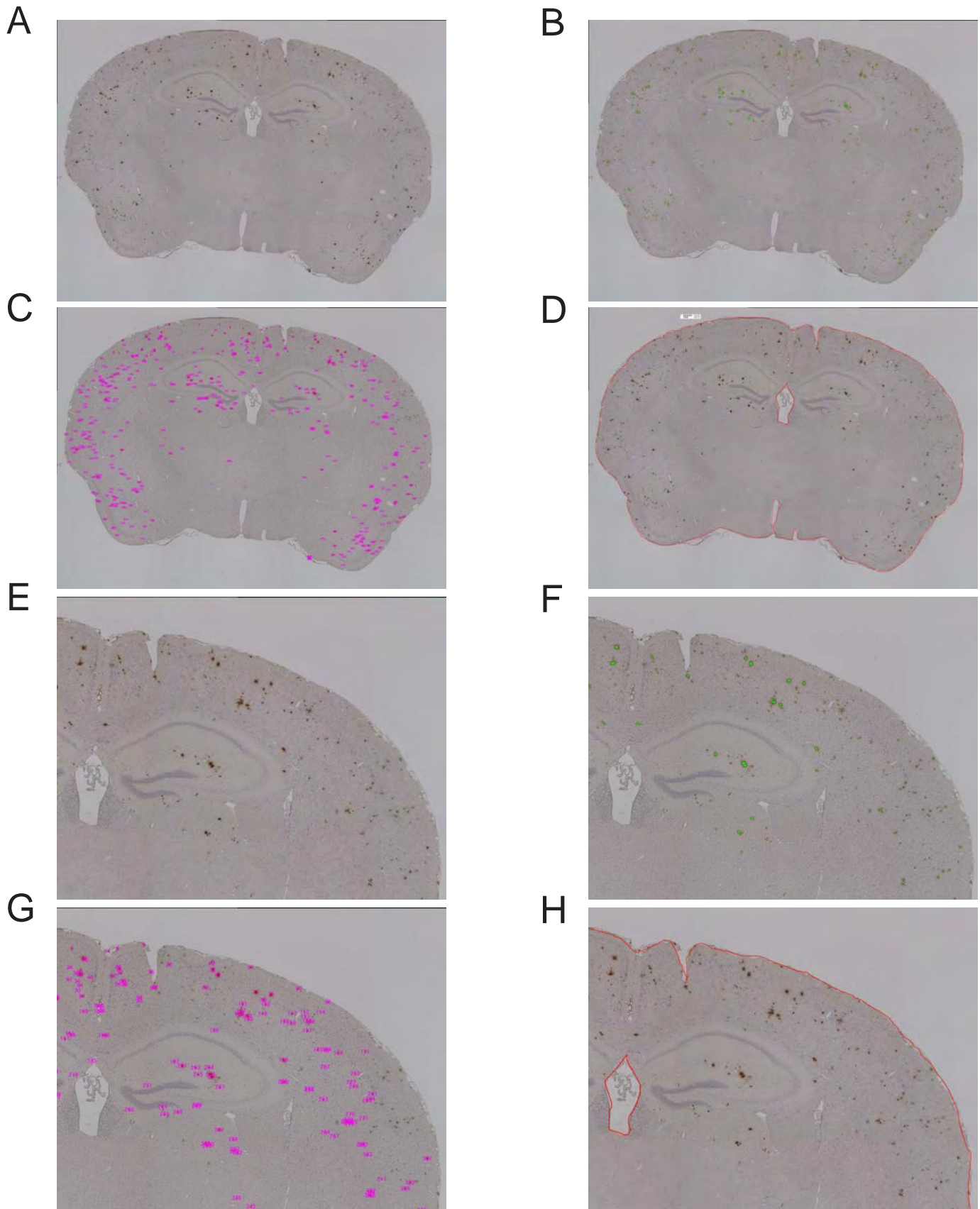IP/ADAM10
(HA)

V5

HA

TCL

NRDc (V5)

β-actin

<Figure4> Ohno M. et al.

<Figure5> Ohno M. et al.

A. Pictures of Aβ immunostained sections were taken by a digital microscope (Keyence BZ9000).

Pictures of a whole brain section (three to four serial sections (7μm) at the same bregma level) were obtained

by combining 8-16 pictures at 40x magnitude using the image stitching function of BZ9000.

B and C. Immunostained brown color was automatically extracted by the dedicated software (Dynamic Cell

Count System BZ-HIC) (B), followed by measurements of the plaque number and plaque surface area (C).

D. Whole brain surface area (D, H) was manually traced and measured by the software.

Aβ plaque load was defined as total plaque surface area / whole brain surface area. E, F, G, and H.

Higher magnification views of A, B, C, and D, respectively.
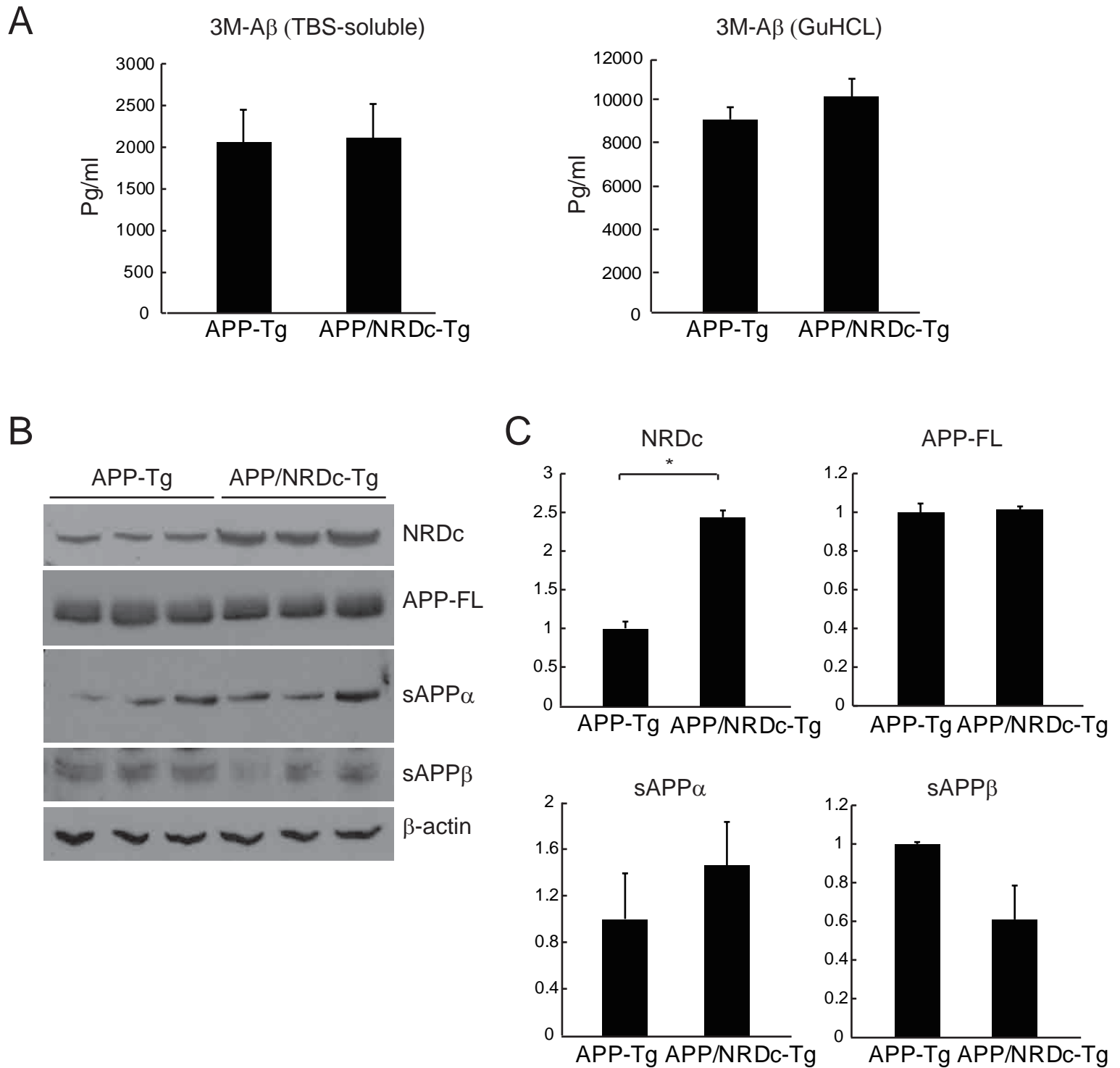
Analysis of 3-month-old pre-deposit mice.

A. Measurement of the Aβ42 peptide in soluble (left panel) and insoluble (right panel) fractions of whole brain extracts by ELISA. n=5/genotype. Data represents the mean +/- s.e.m; no significant difference was observed between APP-Tg and APP/NRDc-Tg mice.

B. Immunoblot analysis of the forebrain extracts of APP-Tg and APP/NRDc-Tg mice. n=3/genotype.

C: Densitometric analysis of the immunoblot shown in B. Data represents the mean +/- s.e.m. *p<0.01.